ACS APPLIED MATERIALS & INTERFACES

RESEARCH ARTICLE

www.acsami.org

Sulfonated Polystyrene Fiber Network-Induced Hybrid Proton Exchange Membranes

Yingfang Yao, Liwen Ji, Zhan Lin, Ying Li, Mataz Alcoutlabi, Hechmi Hamouda, and Xiangwu Zhang*

Fiber and Polymer Science Program, Department of Textile Engineering, Chemistry and Science, North Carolina State University, Raleigh, North Carolina 27695-8301, United States

ABSTRACT: A novel type of hybrid membrane was fabricated by incorporating sulfonated polystyrene (S-PS) electrospun fibers into Nafion for the application in proton exchange membrane fuel cells. With the introduction of S-PS fiber mats, a large amount of sulfonic acid groups in Nafion aggregated onto the interfaces between S-PS fibers and the ionomer matrix, forming continuous pathways for facile proton transport. The resultant hybrid membranes had higher proton conductivities than that of recast Nafion, and the conductivities were controlled by selectively adjusting the fiber diameters. Consequently, hybrid membranes fabricated by ionomers, such as Nafion, incorporated with ionic-conducting nanofibers established a promising strategy for the rational design of high-performance proton exchange membranes.

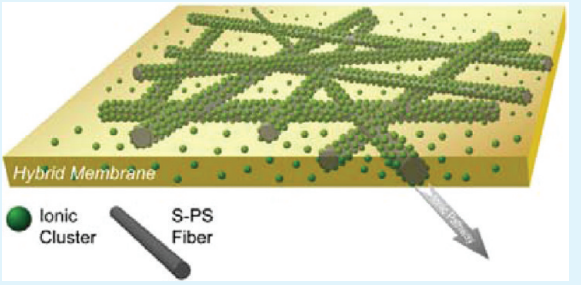

KEYWORDS: hybrid materials, proton exchange membrane, electrospun fibers, sulfonated polystyrene, Nafion

INTRODUCTION

A large number of synthesis and fabrication methods have been demonstrated for generating one-dimensional nanostructures such as fibers, rods, wires, tubes, and so forth.[1,2] Among these methods, electrospinning is one of the most promising technologies to produce continuous nanofibers with diameters ranging from tens of micrometers down to several nanometers at relatively large scale and low cost.[3−14] The advantages of electrospun nanofibers, including small diameter, high surface-to-volume ratio, large porosity, good mechanical property, and diversified architecture and composition, make them potential candidates for applications in areas like catalysis, sensors, hydrogen storage, tissue engineering, drug delivery, bioengineering, functional textiles, etc.

In a typical electrospinning process, a high electric field is applied to the droplet of a viscous polymer solution or melt coming out from the tip of a nozzle. The interaction of the electrical charges with the external electric field causes the pendant droplet to deform into a conical structure called Taylor cone. When electric charges in the fluid surpass the critical value at which the repulsive electrostatic force overcomes the surface tension, a fine charged jet is ejected from the tip of Taylor cone. The charged jet undergoes a whipping motion and is elongated continuously by the electrostatic repulsion until it is deposited onto a grounded collector, resulting in the formation of fine fibers. The formation of fibers is a function of operating parameters, namely voltage, solution feeding rate, and solution properties, such as viscosity, conductivity, surface tension, etc. Consequently, the diameter, architecture, and composition of electrospun fibers can be well controlled by selectively adjusting the processing parameters of electrospinning.

So far, electrospun fibers have been studied as the supporting materials for the electrodes of proton exchange membrane fuel cells (PEMFCs) and direct methanol fuel cells (DMFCs).[15−18] Several advantages have been demonstrated, such as uniform dispersion of fibers in the electrodes and catalyst materials on the fibers and a high accessible area for surface interactions and electron transport. However, only a handful of reports could be found in the application of electrospun fibers in proton exchange membranes, and most of them focused on the polyelectrolyte fibers.[19−22] In these membranes, fibers made of proton conductor, such as Nafion, were incorporated into insulating polymer matrixes. It was reported that, due to the aggregated ionic groups, proton channel structures were formed and led to rapid proton transport.[22] However, the performance (especially, the ionic conductivity) of these polyelectrolyte fiber-incorporated membranes is still unsatisfactory for practical fuel cell applications because of the presence of insulating polymer matrixes.

Herein, we report a novel type of hybrid membrane, in which surface-sulfonated polystyrene (S-PS) electrospun fiber mats were imbedded as a three-dimensional interconnected network into Nafion, a perfluorosulfonic acid ionomer. The embedded fibers with inert cores restrict the swelling of fibers as well as membranes in water and provide good membrane integrity and strength. In addition, the sulfonic acid groups on the fiber surfaces ensure the optimum utilization of percolation pathways for proton transport at the fiber−Nafion interfaces. The newly developed S-PS fiber/Nafion hybrid membranes are easy to fabricate, highly controllable, and can be used in practical fuel cell systems, which offer a promising strategy on the rational design of high-performance proton exchange membranes.

Received: July 12, 2011
Accepted: August 12, 2011
Published: August 12, 2011

EXPERIMENTAL SECTION

Preparation of S-PS Nanofibers. Electrospinning solutions were prepared by dissloving 20−30 wt % polystyrene (PS, M_w = 230 000, Sigma-Aldrich) in a blend solvent of tetrahydrofuran (THF, Sigma-Aldrich) and *N*,*N*-dimethylformamide (DMF, Sigma-Aldrich) (weight ratio: 1:4). The solutions were then electrospun at 12 kV with a feed rate of ~1.0 mL/h. Electrospun fiber mats were collected on the aluminum collector placed at a distance of 15 cm from the electrospinning nozzle.

The as-spun fibers were first cold pressed with a pressure of 380 psi to acquire fiber mats with higher volume density and then soaked into excessive 10 M H_2SO_4 for 24 h at 100 °C to anchor the sulfonate groups. After that, the obtained S-PS fiber mats were rinsed in deionized water 6 times and dried in a vacuum oven at 60 °C for 8 h.

Fabrication of S-PS Fiber/Nafion Hybrid Membranes. S-PS fiber/Nafion hybrid membranes were fabricated by the casting method. During the process, 7.5% Nafion solutions (Dupont, EW = 1100 g·mol^{-1}) were added to S-PS fiber mats. After degassing, the solutions were heated at 60 °C for 8 h and then postcured at 120 °C for 2 h under N_2 to form S-PS fiber/Nafion hybrid membranes. The fiber volume fraction of the hybrid membranes was 10%. For comparison, recast Nafion films were also prepared without the presence of fiber mats.

Membrane Characterization. The nanostructure of the hybrid membranes was determined using field emission scanning electron microscopy (FESEM, JEOL JSM-6400F). The distribution of ionic clusters in S-PS fibers and hybrid membranes was observed with a transmission electron microscopy (TEM, Hitachi HF-2000). Before TEM imaging, both S-PS fibers and hybrid membranes were stained with sodium ions for the clear observation of the ionic clusters by dipping the samples into 1 M NaOH solution for 24 h and then rinsed thoroughly in distilled water. Fourier transform infrared spectra (FT-IR) of PS and S-PS fibers were performed using a Nicolet Nexus 470 spectrometer in the range of 4000−400 cm^{-1}.

Ion Exchange Capacity Measurement. The IEC values of the membranes in acid form were measured by the classical titration technique. Membranes in the acidic form were immersed in 40 mL of 1.0 M NaCl solution for 24 h. Solutions were titrated with 1 M NaOH solution until pH = 7. The IEC was calculated according to the equation:

$$IEC(mequiv/g) = (V_{NaOH} \times C_{NaOH})/W_d$$

where V_{NaOH} and C_{NaOH} are the volume and molar concentrations of NaOH solution, respectively.

Water Uptake Measurement. Both recast Nafion and S-PS fiber/Nafion hybrid membranes were dried in vacuum for 4 h at 60 °C giving the weight of dry membranes and then immersed in deionized water at room temperature for 24 h giving the weight of hydrated membranes. The water uptake was calculated using the following equation:

$$Water\ uptake = \frac{W_w - W_d}{W_d}$$

where W_d and W_w are the weights of the dry and hydrated samples, respectively.

Proton Conductivity Measurement. The resistances of the membranes (size: 2 cm ×2 cm, thickness: 150 μm) were measured using the two-probe impedance method over the frequency range of 1 Hz to 1 MHz on a potentiostat (Gamry Instruments Reference 600). The relative humidity (RH, 20−100%) and temperature (20−100 °C) were controlled in a temperature/humidity chamber (Ransco RTH-600-S). The in-plane proton conductivity (σ) was calculated according to the equation:

$$\sigma = L/RA$$

where L is the distance between the two electrodes, R is the resistance of the membrane, and A is the cross-sectional area of the membrane.

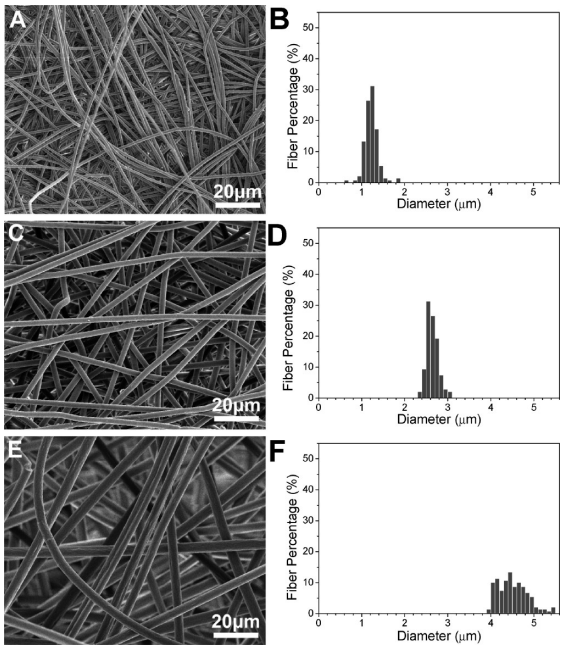

Figure 1. SEM images and histograms of fiber diameter distribution of electrospun PS fibers with different average diameters of (A, B) 1.23 μm, (C, D) 2.65 μm, and (E, F) 4.51 μm. The fiber diameter was controlled via adjusting the PS concentration of pre-electrospinning solution: (A, B) 20%, (C, D) 25%, and (E, F) 30%. Each histogram was plotted with the measurement of more than 150 fibers.

RESULTS AND DISCUSSION

Preparation and Structure of S-PS Fiber Mats. PS fibers were first prepared using the electrospinning method. After electrospinning, the fiber mats were compressed under pressure to increase the volume fraction of fibers. The as-spun fiber mats have a fiber volume fraction of around 5%, and the fiber volume fraction increases to 10% in compressed fiber mats. The thickness of the compressed fiber mats is around 150 μm, which could be changed by adjusting the amount of fibers collected during electrospinning. SEM images and diameter distributions of electrospun PS fiber mats are shown in Figure 1. The fiber diameters were controlled by selectively adjusting the PS concentrations of pre-electrospinning solutions. It is seen that pre-electrospinning solution with lower concentration can produce fibers with smaller diameters. When the concentration increases from 20 to 25 and 30%, the average fiber diameter increases from 1.23 to 2.65 and 4.51 μm, respectively.

The compressed PS fiber mats were then sulfonated in 10 M H_2SO_4. To create a network of interconnecting protonic pathways, the sulfonation was carried out at 100 °C (higher than the glass transition temperature) to bond the neighboring fibers. Figure 2 shows the SEM images and diameter distributions of S-PS fiber mats after sulfonation. It is seen that all samples still keep the fiber structure. However, the neighboring fibers become interconnected with each other, and the fiber diameter decreases to 0.98, 2.21, and 3.60 μm, respectively, for fiber mats produced from 20, 25, and 30% solutions. A possible explanation is that some of the polymer chains on the fiber surface were fully sulfonated to polystyrene sulfonic acid and dissolved into the H_2SO_4 solution during the sulfonation process. Furthermore, because of the interconnections between neighboring fibers, the

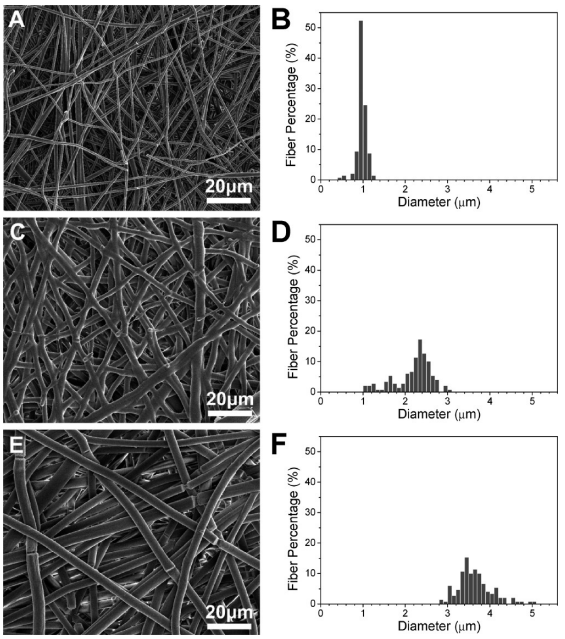

Figure 2. SEM images and histograms of fiber diameter distribution of S-PS fibers with different average diameters of (A, B) 0.98 μm, (C, D) 2.21 μm, and (E, F) 3.60 μm. Each histogram was plotted with the measurement of more than 150 fibers.

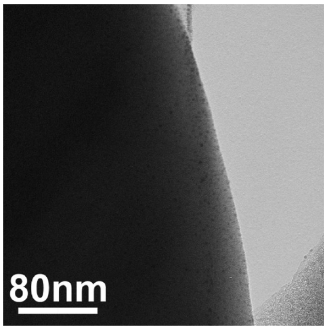

Figure 3. TEM image on the cross-sectional view of a single S-PS fiber. The fiber was stained with sodium ions for clear observation of the distribution of ionic clusters on the fiber.

fiber mats still had a good mechanical integrity and were free-standing after sulfonation.

TEM image of the cross-sectional view on a single S-PS fiber with the diameter of around 3.60 μm is shown in Figure 3. In order to clearly observe the distribution of functional groups, the fiber was stained with sodium ions. In the resultant TEM image, the dark dots represent the ionic domains, i.e., functional groups. It can be clearly observed that most functional groups are distributed on the fiber surface, indicating the surface functionalization of S-PS fibers.

Fourier transform infrared (FT-IR) spectra of both PS and S-PS fiber mats are represented in Figure 4. It is seen that S-PS fiber mats have sulfonic acid group bands at 1178, 1129, and 1035 cm^{-1},[23] which cannot be found from the unsulfonated PS fibers. This indicates the successful formation of S-PS by the sulfonation process. Due to the presence of sulfonic acid groups, the surface of the S-PS fibers is hydrophilic.

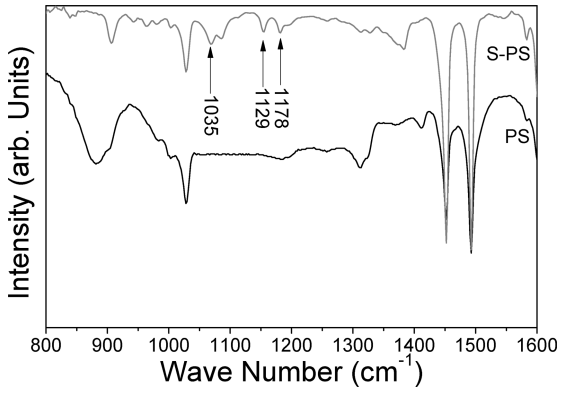

Figure 4. FT-IR spectra of PS and S-PS fiber mats.

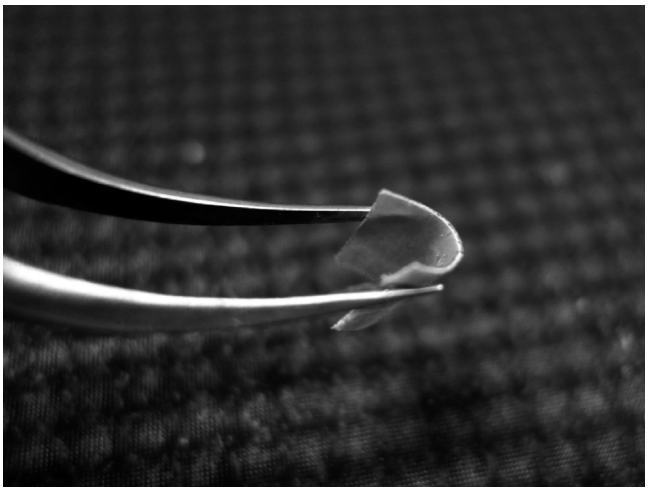

Figure 5. Photograph of a free-standing, flexible S-PS fiber/Nafion hybrid membrane held with a tweezer.

Preparation and Structure of S-PS fiber/Nafion Hybrid Membranes. S-PS fiber/Nafion hybrid membranes were then fabricated by embedding compact S-PS fiber mats in Nafion through the casting method. Figure 5 shows a photograph of an S-PS fiber/Nafion hybrid membrane, in which the fiber diameter is 0.98 μm and the fiber volume fraction is 10%. It is seen that the hybrid membrane is free-standing and flexible. The appearance of the hybrid membranes to naked eyes does not change when the fiber diameter changes. In addition, after conductivity measurements, the hybrid membranes kept their integrity and were still free-standing, illustrating a reasonable mechanical stability with changing humidity and temperature.

Figure 6 shows both the top and cross sectional views of an S-PS fiber/Nafion hybrid membrane, in which the S-PS fiber diameter is 0.98 μm. No obvious defects can be found on the surface of the hybrid membrane (Figure 6A). The fibers are clearly seen from the cross-sectional view of the membrane, with uniformly dense polymeric Nafion filling the voids between fibers (Figure 6B,C), verifying the formation of S-PS fiber/Nafion hybrid membranes.

Proton Conductivities of S-PS Fiber/Nafion Hybrid Membranes. Proton conductivity measurement was performed on S-PS fiber/Nafion hybrid membranes with different diameters of S-PS fibers, and the results are shown in Figure 7. For comparison,

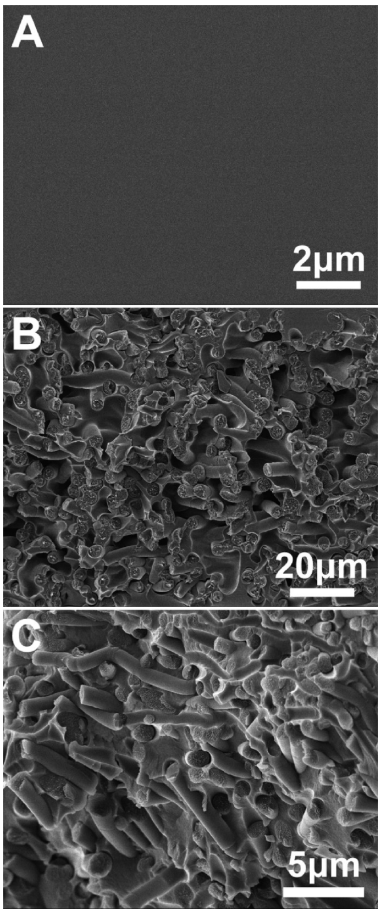

Figure 6. SEM images of (A) top view and (B, C) cross sectional view on a typical S-PS fiber/Nafion hybrid membrane.

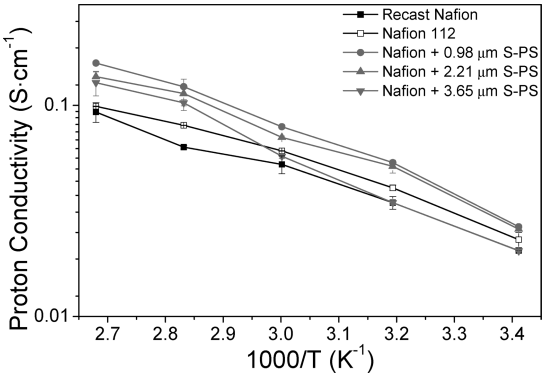

Figure 7. Temperature-dependent proton conductivities of recast Nafion, Nafion 112, and S-PS fiber/Nafion hybrid membranes with different fiber diameters at 80% RH.

the conductivities of recast Nafion are also shown. It is seen that all S-PS fiber/Nafion membranes have higher conductivities than recast Nafion over the entire temperature range. In addition, with a decrease in fiber diameter, the conductivities of S-PS fiber/Nafion hybrid membranes increase. For example, at 100 °C, the proton conductivities of recast Nafion, Nafion 112, and S-PS fiber/Nafion hybrid membranes with fiber diameter of 3.60, 2.21, and 0.98 μm are 9.2×10^{-2}, 9.9×10^{-2}, 1.3×10^{-1}, 1.4×10^{-1}, and 1.6×10^{-1} S·cm^{-1}, respectively.

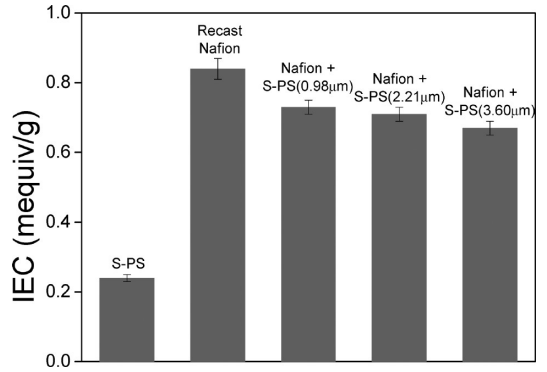

Figure 8. IEC values of S-PS, recast Nafion, and S-PS fiber/Nafion hybrid membranes with different fiber diameters.

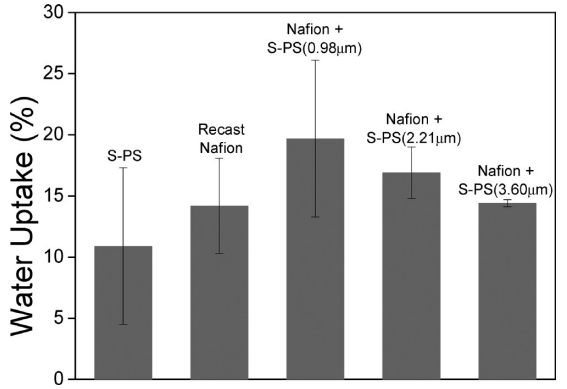

Figure 9. Water uptake values of S-PS, recast Nafion, and S-PS fiber/Nafion hybrid membranes with different fiber diameters.

In most reported proton exchange membranes, the proton conductivity is strongly related to the amount of sulfonic acid groups, and membranes with more sulfonic acid groups typically have higher proton conductivity.[20,21] Figure 8 shows the ion exchange capacities (IECs) of S-PS fibers, recast Nafion, and S-PS fiber/Nafion hybrid membranes with different fiber diameters. It is seen that recast Nafion has a relatively high IEC of 0.84 mequiv/g and S-PS fibers only have a low IEC of 0.24 mequiv/g. The low IEC value of S-PS fibers is mainly because the sulfonation mainly occurs at the fiber surface and the fiber core does not contain a significant amount of sulfonic acid groups. From Figure 8, it is seen that all three S-PS fiber/Nafion hybrid membranes have IEC values between recast Nafion and S-PS fibers. Since the IECs of S-PS fiber/Nafion hybrid membranes are lower than that of Nafion, the enhanced proton conductivities of hybrid membranes are unlikely caused by the increased amount of sulfonic acid groups.

Figure 9 shows the water uptakes of S-PS fibers, recast Nafion, and S-PS fiber/Nafion hybrid membranes with different fiber diameters. It is seen that S-PS and recast Nafion have water uptake of 10.9% and 14.2%, respectively. All three S-PS fiber/Nafion hybrid membranes have water uptakes that are greater than those of S-PS fibers and recast Nafion. Since the hybrid membranes have smaller IEC values than recast Nafion (Figure 8), their high water uptakes are also not caused by the increased amount of sulfonic acid groups. A probable explanation is that, due to the

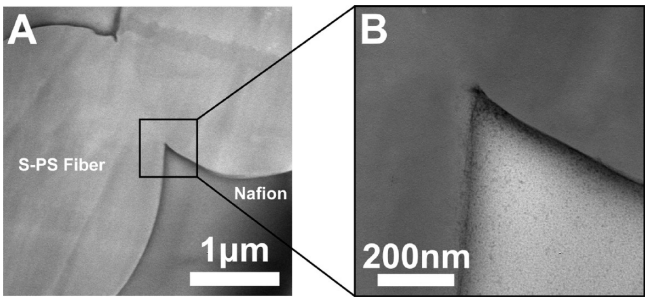

Figure 10. TEM images of (A) the cross-sectional view of a hybrid S-PS fiber/Nafion membrane (D = 3.60 μm) and (B) that with higher magnification. The membrane was stained by sodium ions for clear observation of ionic clusters.

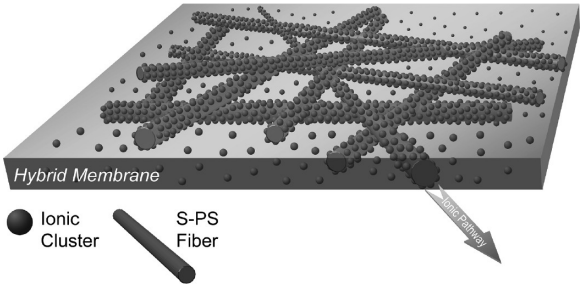

Figure 11. Schematic diagram of S-PS fiber/Nafion hybrid membrane, in which S-PS fibers are wrapped with Nafion matrix and ionic pathways are formed on the fiber−Nafion interface with aggregated ionic clusters.

attraction of sulfonic acid groups on the fiber surfaces, a significant amount of protogenic groups of Nafion aggregate along the S-PS fiber length, forming long-range ionic pathways, which in turn have better capacity to hold water molecules. The long-range ionic pathways formed by the aggregated protogenic groups also improve the proton transport across the membranes, leading to increased conductivities of S-PS fiber/Nafion hybrid membranes. In this work, TEM images of S-PS fiber/Nafion hybrid membranes were obatined to investigate the mechanism of long-range ionic pathways, as discussed below.

TEM Images of Hybrid Membranes. During the formation of hybrid membranes, phase separation between the hydrophobic backbones and the hydrophilic side chains of Nafion causes the formation of ionic clusters.[24−28] Figure 10 shows cross-sectional TEM images of the S-PS fiber/Nafion hybrid membrane, in which the fiber diameter is 3.60 μm. The formation of ionic clusters can be seen from the dark dots in the TEM images. From Figure 10, it is also seen that two neighboring fibers are connected without obvious boundary between them, which illustrates the formation of the network of interconnected fibers. The ionic clusters of the fibers are mainly aggregated on the surface region of the fibers, while few of them can be observed at the inner part of the fibers, indicating the surface functionalization of S-PS fibers. Furthermore, there is a much higher density of ionic clusters on the fiber−Nafion interface than that in the bulk Nafion. This is related to the hydrophilic surface of S-PS fibers. During the formation of hybrid membranes, hydrophilic attractions between functional groups lead to the aggregation of ionic clusters of Nafion onto the interface. Consequently, the large amount of ionic clusters at the interface region forms long-distance ionic pathways along the interconnected S-PS fibers that ensure the effective

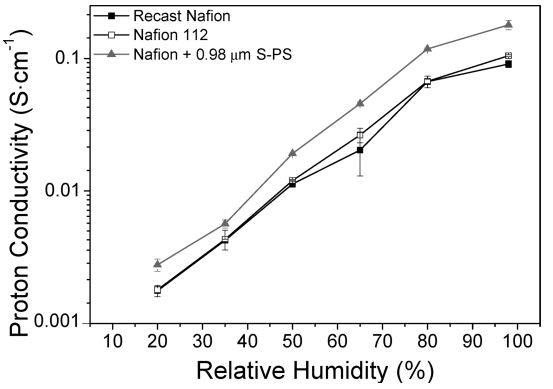

Figure 12. Humidity-dependent proton conductivities of recast Nafion, Nafion 112, and S-PS fiber (0.98 μm)−Nafion hybrid PEM at the temperature of 80 °C.

proton transport through the entire membrane, as shown schematically in Figure 11. As a result, the incorporation of S-ZrO_2 nanofibers into Nafion can effectively improve the proton conductivity without increasing the IEC value.

Effect of Relative Humidity. The proton conductivities of recast Nafion and S-PS fiber/Nafion hybrid membrane (fiber diameter = 0.98 μm) were measured at different RH at 80 °C, as illustrated in Figure 12. It is apparent that the hybrid membrane possesses higher proton conductivities than recast Nafion over the entire RH range. For example, at 100% RH, the proton conductivities of hybrid PEM, Nafion 112, and recast Nafion are 1.8×10^{-1}, 1.0×10^{-1}, and 9.1×10^{-2} S·cm^{-1}, respectively. This clearly demonstrates the beneficial effect of S-PS fibers on the conductivity improvement of hybrid membranes.

CONCLUSIONS

A novel type of S-PS fiber/Nafion hybrid membrane has been developed by incorporating a network of interconnected S-PS fibers into Nafion. With the assistance of continuous S-PS fibers, long-range ionic pathways are formed and play a primary role in the improvement of proton conductivity. A high proton conductivity of 1.8×10^{-1} S·cm^{-1} was observed at 80 °C and 100% RH when the fiber diameter was 0.98 μm. The hybrid membranes comprised with networks of long-range ionic pathways are easy to fabricate, are highly controllable, and can be used in practical fuel cell systems. Furthermore, this type of fiber-induced hybrid membranes can also be useful for other purposes, such as electrodialysis separations, sensors, and industrial electrolyses.

AUTHOR INFORMATION

Corresponding Author

*Phone: 919-515-6547. E-mail: xiangwu_zhang@ncsu.edu.

ACKNOWLEDGMENT

The authors wish to acknowledge the National Science Foundation for funding this research.

REFERENCES

(1) Xia, Y.; Yang, P.; Sun, Y.; Wu, Y.; Mayers, B.; Gates, B.; Yin, Y.; Kim, F.; Yan, H. *Adv. Mater.* **2003**, *15*, 353–389.

(2) Hu, J.; Odom, T. W.; Lieber, C. M. *Acc. Chem. Res.* **1999**, *32*, 435–445.

(3) Dzenis, Y. *Science* **2004**, *304*, 1917–1919.
(4) Lin, D.; Xia, Y. *Adv. Mater.* **2004**, *16*, 1151–1170.
(5) Huang, Z.-M.; Zhang, Y.-Z.; Kotakic, M.; Ramakrishna, S. *Compos. Sci. Technol.* **2003**, *63*, 2223–2253.
(6) Teo, W. E.; Ramakrishna, S. *Nanotechnology* **2006**, *17*, R89–R106.
(7) Ramakrishna, S.; Fujihara, K.; Teo, W.-E.; Yong, T.; Ma, Z.; Ramaseshan, R. *Mater. Today* **2006**, *9*, 40–50.
(8) Greiner, A.; Wendorff, J. H. *Angew. Chem., Int. Ed.* **2007**, *46*, 5670–5703.
(9) Thavasi, V.; Singh, G.; Ramakrishna, S. *Energy Environ. Sci.* **2008**, *1*, 205–221.
(10) Agarwal, S.; Wendorff, J. H.; Greiner, A. *Macromol. Rapid Commun.* **2010**, *31*, 1317–1331.
(11) Yao, Y.; Gu, Z. Z.; Zhang, J.; Pan, C.; Zhang, Y.; Wei, H. *Adv. Mater.* **2007**, *19*, 3707–3711.
(12) Feng, Z. Q.; Chu, X. H.; Huang, N. P.; Leach, M. K.; Wang, G.; Wang, Y. C.; Ding, Y. T.; Gu, Z. Z. *Biomaterials* **2010**, *31*, 3604–3612.
(13) Ji, L. W.; Zhang, X. W. *Electrochem. Commun.* **2009**, *11*, 1146–1149.
(14) Ma, M.; Titievsky, K.; Thomas, E. L.; Rutledge, G. C. *Nano Lett.* **2009**, *9*, 1678–1683.
(15) Steigerwalt, E. S.; Deluga, G. A.; Cliffel, D. E.; Lukehart, C. M. *J. Phys. Chem. B* **2001**, *105*, 8097–8101.
(16) Liu, F.-J.; Huang, L.-M.; Wen, T.-C.; Gopalan, A. *Synth. Met.* **2007**, *157*, 651–658.
(17) Gharibi, H.; Zhiani, M.; Entezami, A. A.; Mirzaie, R. A.; Kheirmand, M.; Kakaei, K. *J. Power Sources* **2006**, *155*, 138–144.
(18) Yuan, F.; Ryu, H. *Nanotechnology* **2004**, *15*, S596–S602.
(19) Chen, H.; Snyder, J. D.; Elabd, Y. A. *Macromolecules* **2008**, *41*, 128–135.
(20) Dong, B.; Gwee, L.; Cruz, D. S.; Winey, K. I.; Elabd, Y. A. *Nano Lett.* **2010**, *10*, 3785–3790.
(21) Choi, J.; Lee, K. M.; Wycisk, R.; Pintauro, P. N.; Mather, P. T. *Macromolecules* **2008**, *41*, 4569–4572.
(22) Tamura, T.; Kawakami, H. *Nano Lett.* **2010**, *10*, 1324–1328.
(23) Bekri-Abbesa, I.; Bayoudhb, S.; Baklouti, M. *Desalination* **2008**, *222*, 81–86.
(24) Hsu, W. Y.; Gierke, T. D. *J. Membr. Sci.* **1983**, *13*, 307–326.
(25) Mauritz, K. A.; Rogers, C. E. *Macromolecules* **1985**, *18*, 483–491.
(26) Orfino, F. P.; Holdcroft, S. *J. New Mater. Electrochem. Syst.* **2000**, *3*, 287–290.
(27) Gebel, G. *Polymer* **2000**, *41*, 5829–5838.
(28) Schmidt-rohr, K.; Chen, Q. *Nat. Mater.* **2008**, *7*, 75–83.